

# Investigations on Thermal, Structural and Morphological Properties of $Ba_{1-x}Sr_xTiO_3$

R. Balaji<sup>1</sup>, K. Abduraof<sup>2</sup>, A.Senthilkumar<sup>3</sup>  
{rbi.phy@psgtech.ac.in<sup>1</sup>, abdulrahoof87@gmail.com<sup>2</sup>, ask.apsc@psgtech.ac.in<sup>3</sup>}

Department of Physics, PSG College of Technology, Coimbatore-04, TN<sup>1</sup>, Department of Physics, MSTM Arts and Science college, Calicut University, Perinthelmana, Kerala<sup>2</sup>, Department of Applied Science (Physics), PSG College of Technology, Coimbatore-04, TN<sup>3</sup>.

**Abstract:** Barium Strontium Titanate (BST), with the general formula  $Ba_{1-x}Sr_xTiO_3$  hold perovskite phase of Tetragonal Tungsten Bronze (TTB) structure was considered as promising lead-free ferroelectric material. DSC, XRD, HRTEM and SEM analysis confirms the calcination temperature, phase purity, particle size and microstructure of the barium strontium titanate ferroelectric materials prepared. Unlike other materials, the BST exhibits ferroelectricity over wide composition range  $0.01 \leq x \leq 0.30$  and  $0.20 \leq x \leq 0.80$ , respectively. It delivers an opportunity to design BST based ferroelectric with desired properties to meet the requirements of device fabrication such as phase shifters and voltage-controlled oscillators.

**Keywords:** Barium Strontium Titanate, DSC, XRD, HRTEM, SEM, ferroelectric material.

## 1. Introduction

Barium Strontium Titanate (BST) was considered as a promising ferroelectric material with excellent thermal stability and high dielectric constant promotes diverse applications such as piezoelectric, pyroelectric sensors and multilayer ceramic capacitors, dynamic random-access memories (DRAM). Moreover, the BST materials exhibit different Curie temperature ( $T_c$ ) at various Ba/Sr ratio which reveals the tunable composition range of Ba and Sr [1].

The dielectric properties change with variation in  $T_c$ . Consequently, fabrication of BST with desired high dielectric constant would be simple which enhance its wide range of applications [2]. However, to achieve high dielectric constant, the grains size should be reduced to some extent. On the other hand, preparations of materials with smaller grains are always difficult in conventional sintering. This may be due to slow ramping rate and heterogeneous temperature absorption as a result of energy transfer.

The microwave assisted sintering requires extremely less time compared with conventional sintering process where the time required to prepare BST perovskite phase at  $1400^\circ\text{C}$  was 20 minutes [3,8]. In this process, the heat is produced internally within the material by the absorption of microwave energy. The heating of the materials is very rapid as by gaining heat by means energy conversion instead of energy transfer, which occurs in the

conventional technique. Further, rapid heating rates ( $> 400^{\circ}\text{C}/\text{min}$ ) and excellent mechanical properties caused by fine microstructures improve the significance of microwave sintering [4]. In this study, BST materials of six different compositions were prepared in the ferroelectric region named as BST 05, BST 10, BST 15, BST 20, BST 25, BST 30.

## **2. Experimental Method**

### **2.1. Preparation of lead-free BST**

The precursors, Strontium Nitrate, Barium Nitrate and Titanium dioxide were used to synthesize various compositions of  $\text{Ba}_{1-x}\text{Sr}_x\text{TiO}_3$  (BST), where  $x = 0.05, 0.10, 0.15, 0.20, 0.25$  and  $0.30$  and the samples with various  $x$  values and they are christened as BST05, BST10, BST15, BST20, BST25 and BST30, respectively. The Barium Strontium Titanate (BST) ferroelectric materials was experimentally prepared through solid state reaction method. The synthesis procedure of BST was similar except their calcination and sintering temperature. Stoichiometrically prepared powders were wet mixed and dried at  $100^{\circ}\text{C}$ . The calcination was carried out at  $1100^{\circ}\text{C}$  for BST samples. The calcination duration was fixed at 6 hours. The green pellets were prepared with diameter of 12 mm and 2 mm thickness using a uni-axial hydraulic pellet press at 10 MPa.

### **2.2. Microwave sintering of lead-free BST**

Barium Strontium Titanate (BST) pellets were sintered using microwave furnace at  $1400^{\circ}\text{C}$  with duration of 20 minutes. The calcined powder and sintered BST samples were characterized for structural analysis using Shimadzu, Japan / 6000 X-Ray diffractometer and the densities of all the BST samples were measured by using Archimedes principle [9]. Surface morphologies of the BST samples were recorded using (JEOL / JSM 6390) scanning electron microscope (SEM) and reported.

## **3. Result and Discussion**

### **3.1 DIFFERENTIAL SCANNING CALORIMETRY (DSC)**

Thermogravimetry (TG) curves for all BST compositions analyzed using DSC (Netzsch, Germany, STA449C/4/MFC/G). Figure.1 shows the Differential Scanning Calorimetry (DSC) results of all the BST samples. The sample measurements were recorded from room temperature to the maximum of  $1200^{\circ}\text{C}$  at a heating rate of  $10^{\circ}\text{C} / \text{min}$ . The TG curve clearly shows massive weight loss from  $600^{\circ}\text{C}$  to  $700^{\circ}\text{C}$  due to the decomposition of organic compounds [5]. Moreover, it was evident from the endothermic peak observed at  $660^{\circ}\text{C}$  in the DSC curve. However, the secondary phases of BST materials were observed between the calcination temperature of  $700^{\circ}\text{C}$  and  $800^{\circ}\text{C}$  [6]. Therefore, the calcination temperature was considered above  $800^{\circ}\text{C}$ , which extends to  $1100^{\circ}\text{C}$  for the formation of desired BST phase. So, the calcination temperature was fixed at  $1100^{\circ}\text{C}$ .

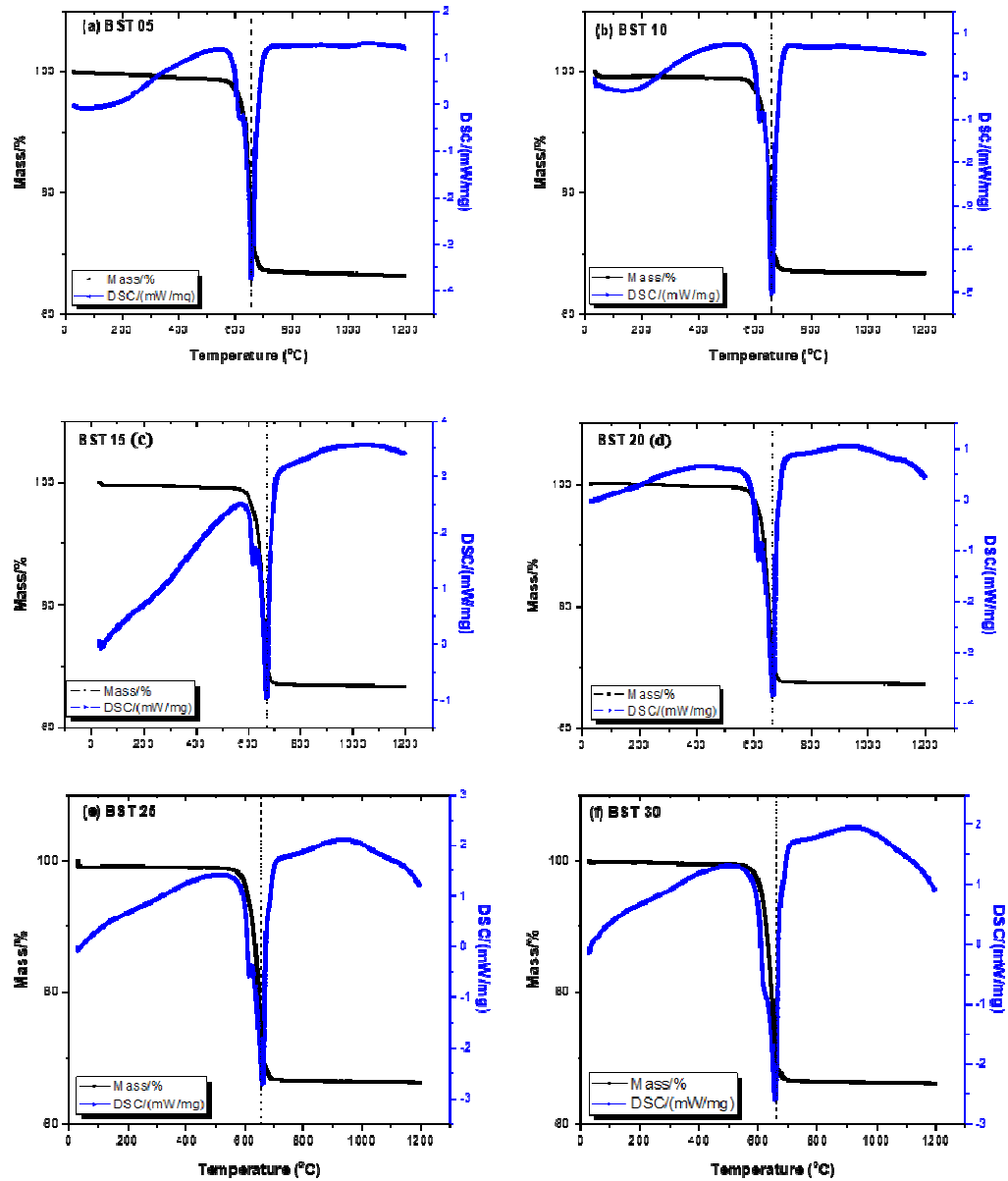
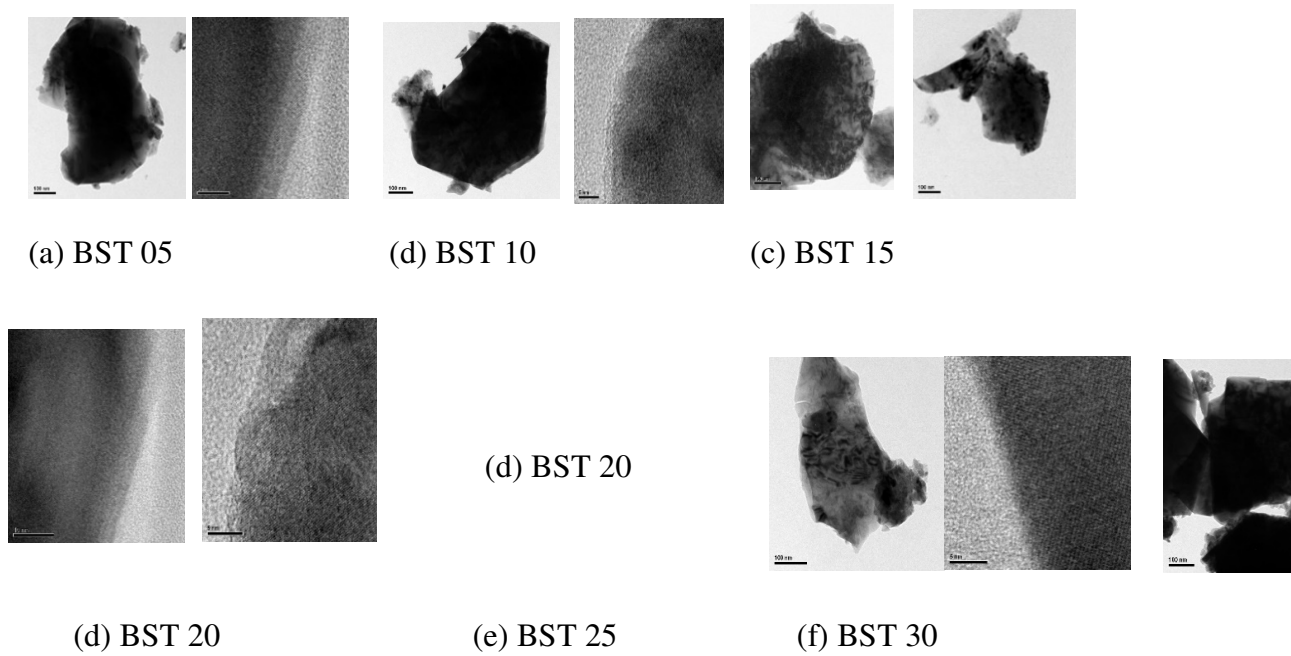


Fig.1 Variation of DSC and TG with temperature for BST (a) BST 05, (b) BST 10, (c) BST 15, (d) BST 20, (e) BST 25, (f) BST 30.

### 3.2 PARTICLE SIZE AND MORPHOLOGY

High Resolution - Transmission Electron Microscopy (HR-TEM) of the BST powder sample calcined at 1100°C were shown in Figure 2 (a, b, c, d, e& f). It was observed that the size of particles for all compositions was approximately below 400nm. In addition, the powders exhibit sharp edges with no degree of agglomeration [7].



**Fig.2 HRTEM image and Lattice image of BST powders ((a) BST 05, (b) BST 10, (c) BST 15, (d) BST 20, (e) BST 25, (f) BST 30.**

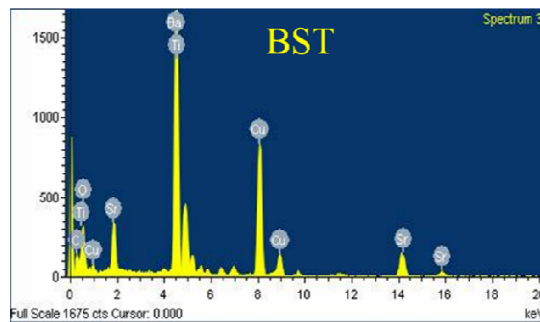


**Fig.3 EDS graphs of BST precursor powders**



In,The Energy Dispersive X-ray spectroscopy (EDS) graph was shown in Figure 3which confirms the presence of Sr, Ba Nb and O elements in the powders.

### 3.3 PHASE ANALYSIS USING XRD

#### 3.3.1Structural Analysis of Calcined Samples

In Figure.4, the XRD peaks are indexed by JCPDF (44-009), and the structure found to be perovskite for all the compositions. Likely, orientations of the grains are major along the direction of (110) plane which favors high dielectric constant [9]. It is to be noted that, the maximum intensity peak positions of BT and ST falls in the same  $2\theta$  values of BST. The increase in Sr or decrease in Ba content in the compositions does not alter the peaks intensity value [10]. This confirms the complete phase formation of BST occurs at a temperature of  $1100^{\circ}\text{C}$  with the absence of individual phases such as BT and ST.

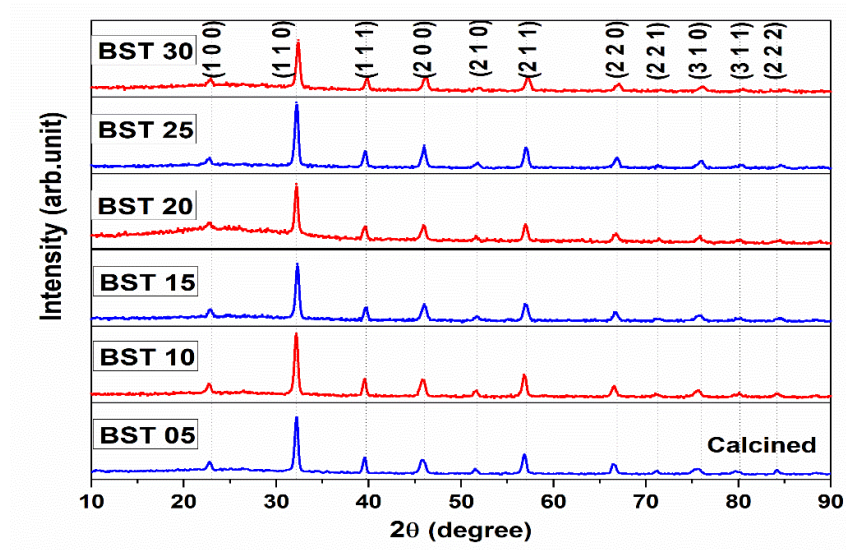


**Fig.4** XRD patterns of BST calcined at  $1100^{\circ}\text{C}$ .

When the sintering temperature reaches  $1200^{\circ}\text{C}$ , it is observed that the perovskite phase formation completed in the samples. The increases in calcination temperature above  $1100^{\circ}\text{C}$  result in agglomeration of particles coupled with the sign of grain growth at an initial stage. As a result, the powders are less reactive for sintering. Also, the formation of grains and agglomeration hampered the density of the green pellet [11].Therefore, the calcination temperature was restricted to  $1100^{\circ}\text{C}$ .

**Table1.** Lattice parameters of BST samples calcined at 1110°C

Sample Name	a (Å)	c (Å)	c/a	Volume (m <sup>3</sup> )
BST 23 (JCPDS - 44-009)	3.9771	3.9883	1.002816	
BST 05	3.979	4.0012	1.005579	6.15*10 <sup>-29</sup>
BST 10	3.9901	4.0098	1.004937	6.15*10 <sup>-29</sup>
BST 15	3.9833	4.0026	1.004845	6.13*10 <sup>-29</sup>
BST 20	3.9987	4.0084	1.002426	6.12*10 <sup>-29</sup>
BST25	3.9967	4.0004	1.000926	6.09*10 <sup>-29</sup>
BST30	4.0114	4.0088	0.999352	6.03*10 <sup>-29</sup>

The lattice parameters of all the calcined BST compositions are shown in Table 1. These parameters are calculated from the plane (110) and (111) peaks of X-ray diffraction patterns of

the samples [12]. It is observed that the increase in Sr content increases the  $c/a$  ratio which indicates the stability of perovskite structure.

### 3.3.2 Structural Analysis of Sintered Samples

Figure 5 shows the XRD patterns of all the sintered BST compositions which confirm the complete perovskite phase formation without the presence of secondary phases such as ST and BT. All these patterns depict the formation of a single phase perovskite structure. The sintering process was carried out at 1400°C using a microwave furnace [9,10]. It was observed that the whole diffusion process in the sample completed within 20 minutes of time duration.

In Table 2, it was clearly observed that, the lattice parameters and percentage of theoretical density for BST05, BST10, BST15, BST20, BST25 and BST30 was calculated as 95.30, 92.93, 93.63, 96.19, 97.93 and 96.06 % respectively. It was clearly understood that the near theoretical densities are achieved for all the compositions [13].

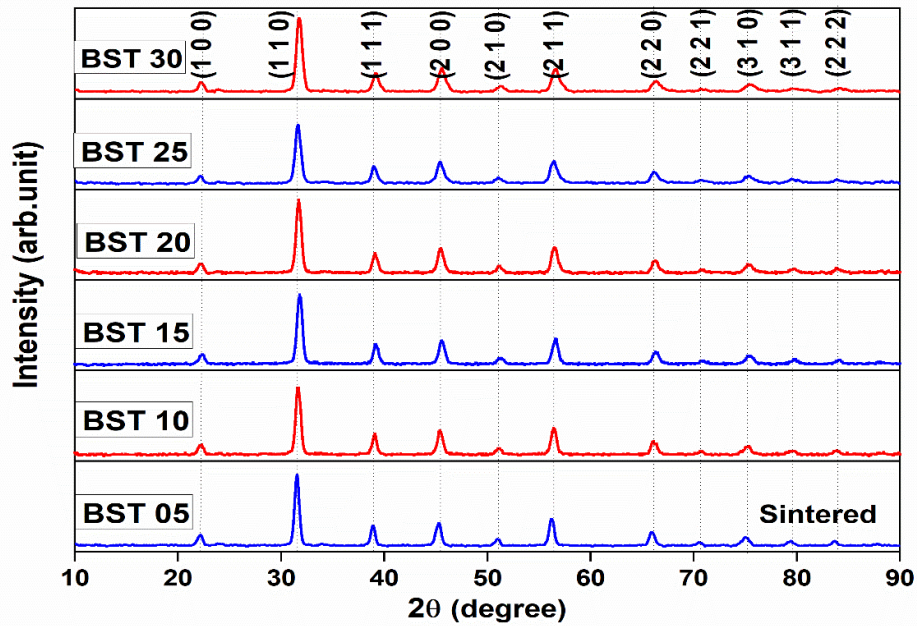


Fig.5. XRD patterns of BST sintered at 1400°C



**Table2.** Lattice parameters and densities of BST compositions sintered at 1400°C

Sample Name	a (Å)	c (Å)	c/a	$\rho_{Th}$ g/cc	$\rho_{exp}$ g/cc	% of $\rho_{Th}$
BST 05	3.9204	3.9637	1.0110	6.2224	5.93	95.30
BST 10	3.9328	3.9733	1.0102	6.3594	5.91	92.93
BST 15	3.9357	3.9702	1.0087	6.2904	5.89	93.63
BST 20	3.9113	3.9436	1.0082	6.0169	5.78	96.06
BST 25	3.9308	3.9620	1.0079	6.0854	5.96	97.93
BST 30	3.9335	3.9622	1.0072	6.1539	5.92	96.19

**Figure.6** Variation of c/a ratio of calcined and sintered BST with Sr content

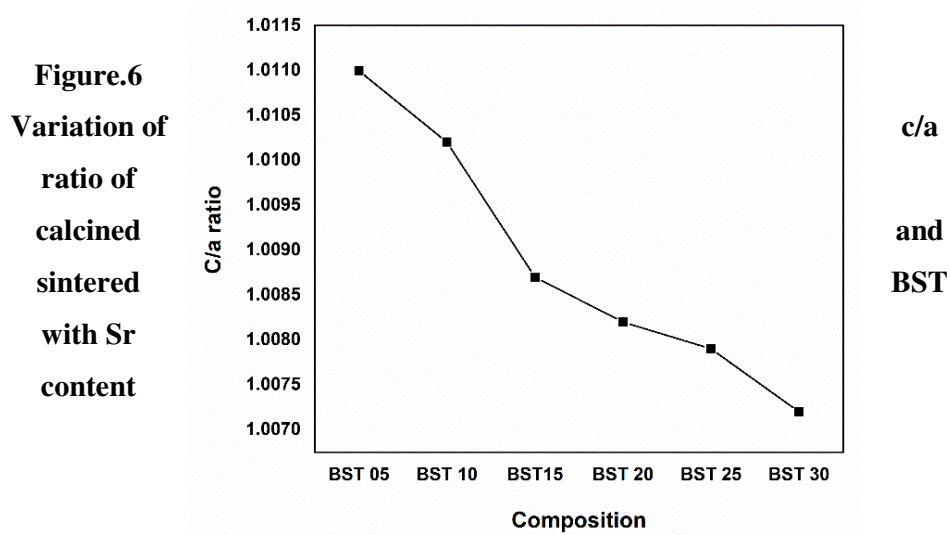


**Figure.6 Variation of c/a ratio of calcined and sintered BST with Sr content**

The variations of c/a ratio of calcined and sintered BST with Sr content are shown in Figure 6. As the Sr content increases, the c/a ratio approaches unity, and the stable tetragonal perovskite structure transforms to a cubic structure. In addition, the c/a ratios of all the sintered BST samples enhance the self-stability of a tetragonal structure [14]. Figure 7 shows the variation of the theoretical density for all BST composition. It is clearly seen that minimal change in densities is observed for all the BST compositions. These small variations may be due to different grain size for different compositions. Further, BST 25 exhibits higher value density, owing to the grains arrangements in well-oriented manner[15]. The repeatability of density results confirms the variation in compositions.

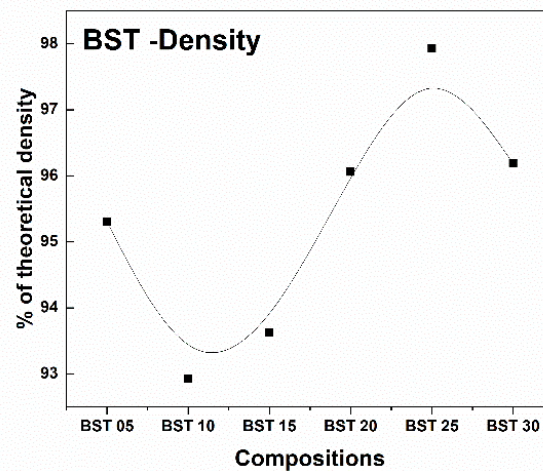


**Fig.7** Variation of theoretical density of BST with compositions

### **3.4 SURFACE MORPHOLOGY STUDIES USING SEM:**

SEM morphology of BST samples, sintered at 1250°C, is shown in Figure 8 (a, b, c, d, e & f). The SEM images clearly exhibit incomplete/ coalesced grain formation indicates inefficient sintering temperature. Further, an increase in Sr content does not change the morphology [16]. Similar results are observed for the same material prepared through conventional sintering for the abnormal grain growth on microstructure[17,18].

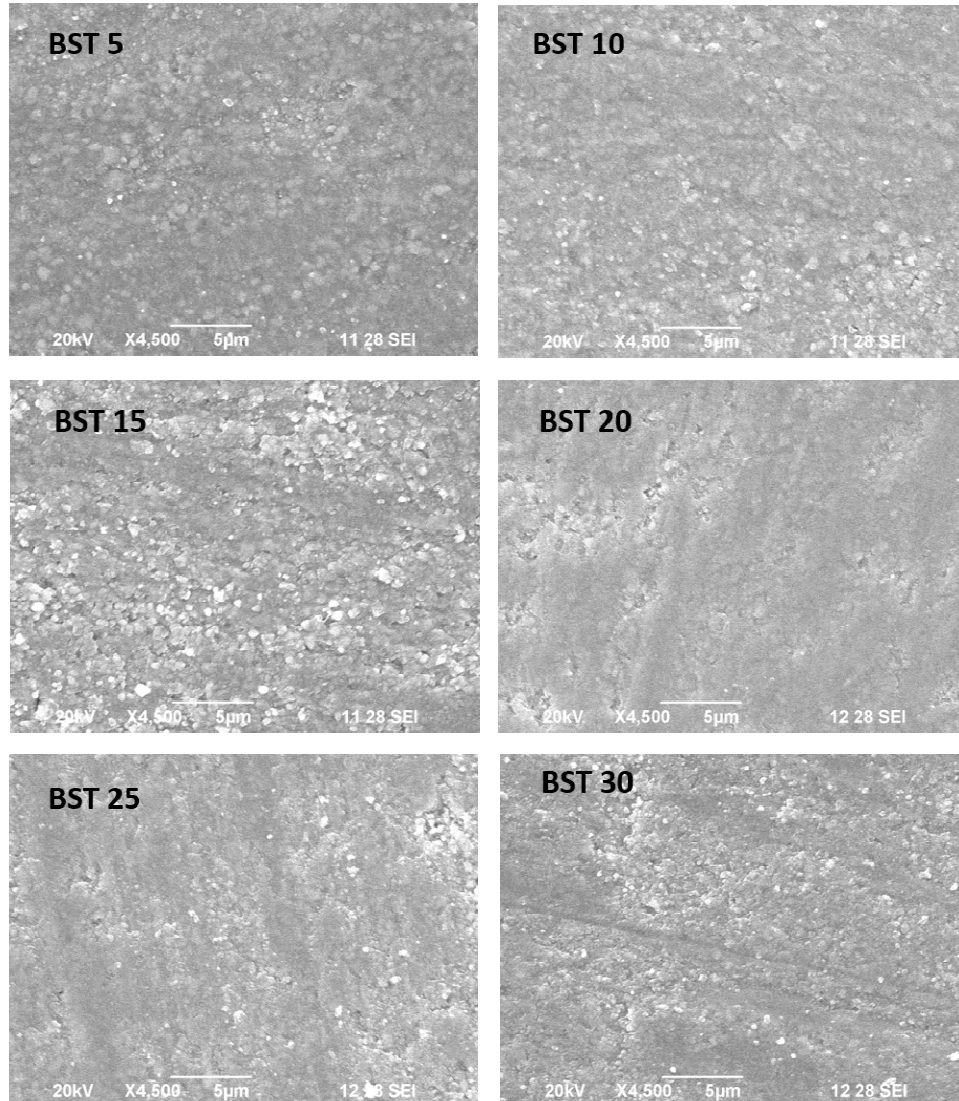


**Fig. 8** SEM image of BST powders ((a) BST 05, (b) BST 10, (c) BST 15, (d) BST 20, (e) BST 25, (f) BST 30).

According to improve the microstructure of BST, the sintering temperature is increased to 1400°C. The morphology of different Sr concentration of BST is shown in Figure.8(a, b, c, d, e & f ). All samples, except BST 25 and BST 30, exhibit similar morphology of anisotropic grain microstructures with pronounced layered/faceted grain microstructure with no coalesced grains [19]. This result is in excellent agreement with the density results obtained using Archimedes principle. The microstructure of the sintered BST compositions with uniform grain distribution represents a development of good microstructure, particles free from aggregate grain growth, pores and duplex microstructure. The average grain sizes measured from the sample were ranged from 3 to 10 µm for all BST compositions [20].

#### 4. CONCLUSIONS

The Barium Strontium Titanate ( $Ba_{1-x}Sr_xTiO_3$ ) perovskite structure with Tetragonal Tungsten Bronze (TTB) structure were successfully synthesized through solid state reaction. The morphology of BST exhibits fine grains for all BST compositions. The intricacy in obtaining the morphology was successfully solved by using microwave treatment. The morphology of BST exhibits Abnormal Grain Growth (AGG) and duplex microstructure free BST for all compositions. The density of sintered BST for all compositions was found to be ~90% of theoretical density. The tunable  $T_c$  behaviour of BST, shown that the prepared BST samples are suitable for tunable microwave device applications.

#### References

- [1] H. S. Nalwa (Ed.) 1999, 'Handbook of Low and High Dielectric Constant Materials and Their Applications', Phenomena, Properties and Applications Academic Press, Vol-2, New-York.
- [2] J. Herbert 1985, 'Ceramic Dielectrics and Capacitors - Electrocomponent Science Monographs', Gordon & Breach Vol. 3., London.
- [3] R. C. Buchanan 1991, "Ceramic Materials for Electronics, Marcel Dekker Inc., New York, 2nd Edition,
- [4] L. M. Levinson (Ed.) 1988, 'Electronic Ceramics', Dekker, New York.
- [5] J. Herbert 1985, 'Ferroelectric Transducers and Sensors', Electro component Science Monographs, Gordon & Breach, Vol. 3, London.
- [6] R. W. Whatmore, J. M. Herbert & F. W. Ainger 1980, 'Recent developments in ferroelectrics for infrared detectors', Phys. Status Solidi A, 61(1), vol.73.
- [7] D. Vonder Linde & A. M. Glass 1975, 'Photorefractive effects for reversible holographic storage of information', Apl. Phys., 8(2), vol.85.
- [8] R. Wroe 1999, Microwave sintering of coming age, Metal powder report, Metal Powder Report, 54(7-8), 24.
- [9] J. D. Katz 1992, Microwave Sintering of Ceramics, Ann. Rev. Mater. Sc., 22, 53.
- [10] D. D. Upadhaya, A. Ghosh, K. R. Gurumurthy 2001, Ram Prasad, Microwave sintering of cubic zirconia, Ceram. Int., 27 (4), 415. Burcu Ertug 2013, 'Overview of the electrical properties of Barium Titanat', American Journal of Engineering Research (AJER), Vol.02, Issue.8, pp 01-07.
- [11] Chen-Feng Kao & Wein-Duo Yang 1999, 'Preparation of Barium Strontium Titanate powder from Citrate Precursor', Applied organometallic chemistry.no.13, pp. 383-397.
- [12] L. Simon-Seveyrat, A. Hajjaji, Y. Emziane, B. Guiffard & D. Guyomar 2007, 'Re-investigation of synthesis of  $BaTiO_3$  by conventional solid-state reaction and oxalate

- coprecipitation route for piezoelectric applications', *Ceramics International*, no.33, pp. 35–40.
- [13] O. Namsar, A. Watcharapasorn & S. Jiansirisomboon 2012, 'Structure–property relations of ferroelectric BaTiO<sub>3</sub> ceramics containing nano-sized Si<sub>3</sub>N<sub>4</sub> particulates', *Ceramics International*, no.38S, pp. S95–S99.
- [14] Sonia, R.K. Patel, P. Kumar, C. Prakash & D.K. Agrawal 2012, 'Low temperature synthesis and dielectric, ferroelectric and piezoelectric study of microwave sintered BaTiO<sub>3</sub> ceramics', *Ceramics International*, no.38, pp.1585–1589.
- [15] Ries\*, A.Z. Simoes, M. Cilense, M.A. Zaghete and J.A. Varela, 'Barium strontium titanate powder obtained by polymeric precursor method', *Materials Characterization* 50 (2003) 217–221.
- [16] S. Leppvuori, T. Hannula And A. Uusimäki, A thick film capacitive temperature sensor using barium strontium titanate glass formulations, *Electrocomponent Science and Technology*. 1979, Vol. 6, pp. 13-18.
- [17] O.P, Thakur, Chandra Prakash & D, K, Agrawal 2002, 'Microwave synthesis and sintering of Ba<sub>0.95</sub> Sr<sub>0.05</sub> TiO<sub>3</sub>', *Materials letters*, Vol. 56, pp. 970-973.
- [18] Chen-Feng Kao\* and Wein-Duo Yang 1999, 'Preparation of Barium Strontium Titanate Powder from Citrate Precursor' *Applied Organometallic Chemistry*, Vol.13, pp. 383–397.
- [19] F.H.We, F.Malek, S.Sreekantan, A.U.Al-amani, F.Ghani and K.Y.You 2011, 'Investigation of the characteristics of Barium strontium Titanate (BST) Dielectric resonator ceramic loaded on array antennas, *Progress in electromagnetic research*, vol. 121, pp. 181-213.
- [20] Teoh Wah Tzu, Zainal Arifin Ahmad and Ahmad Fauzi Mohd Noor 2006, 'Dielectric properties and microstructure of Ba<sub>0.70</sub> Sr<sub>0.30</sub> TiO<sub>3</sub> derived from mechanically activated BaCO<sub>3</sub>-SrCO<sub>3</sub>-TiO<sub>2</sub>, *Zojomo* vol 2